A Novel Variance-based Object Detection scheme for Railroad Ground Penetrating Radar Images

Jitesh Batra [1], Dongming Peng[1] and Robert Palmer [2]

[1]Department of Computer and Electronics Engineering, University of Nebraska – Lincoln
Omaha, Nebraska, USA
dpeng@unl.edu

[2] School of Meteorology, University of Oklahoma (OU)
Norman, Okalahoma, USA
rpalmer@ou.edu

Abstract

A method is presented which detects subsurface objects mapped by ground penetrating radar. An image processing algorithm was developed to automate the process of locating subsurface objects..

Keywords: Ground penetrating radar, Object detection.

1. Introduction

Ground penetrating radar (GPR) [1] uses electromagnetic wave propagation and scattering to image, locate and quantitatively identify changes in electrical and magnetic properties in the ground. Detectability of a subsurface feature depends upon contrast in electrical and magnetic properties, and the geometric relationship with the antenna. Quantitative interpretation through modeling can derive from ground penetrating radar data such information as depth, orientation, size and shape of buried objects, density and water content of soils, and much more. The depth to which radar energy can penetrate and the amount of definition that can be expected in the subsurface is partially controlled by the frequency of the radar energy transmitted. U.S. railroads spend tens of millions of dollars each year for ballast and ballast related maintenance. Track maintenance costs caused by poor subgrade conditions can add millions more than the total maintenance costs. The total damage is about 103 million dollars per year due to track defects [2]. 11.5 percent of these accidents result from problems in the tracks. Due to the sensitivity of GPR to water, the presence of subsurface water pockets and saturated soil conditions can be easily detected [3] [4].

In this paper, GPR is used to detect subsurface pipe-like objects below railway tracks which are important to track safety maintenance. These objects are hard to detect using GPR images which necessitate complicate customized image processing algorithms. In the experiment for this paper this paper, SIR-10B was used which is manufactured by Geophysical Survey Systems, Inc. [6]. The system consists of the following components:

- Model MF-10B Mainframe
- Model CD-10B control / display unit

The mainframe provides antenna interface modules, data collection, signal processing hardware, data storage devices and connectors to external devices. The display unit connects to a video monitor and a keyboard.

2. Object Detection Algorithm

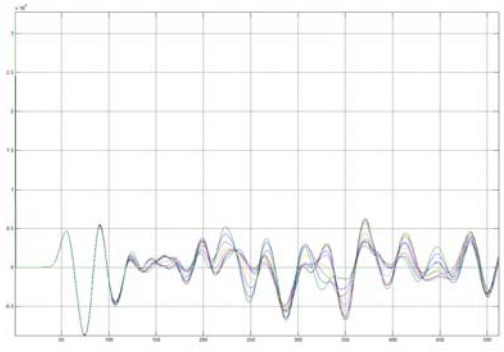

Figure 1: Example of amplitude response over nine scans of a Received signal.

The variance is a measure of how spread out a distribution is. It is computed as the average squared deviation of each number from its mean. Conceptually variance calculates the over all contrast of the image. We can use this ideology to calculate the variance of a particular block of an image. The block size depends on the size of the image and the size of the object (which we are trying to detect or identify). If we calculate the variance in a particular block we will be able to identify the points where the difference in amplitudes is the max. With the process of learning algorithms we will be able to identify points with maximum variance. These points are then identified as probable objects. The GPR system uses a squared, half-wave sinusoid or Gaussian current pulse to excite a dipole antenna [7]. When this Gaussian pulse is transmitted through the ground (subsurface) we get an amplitude response. Figure 1 shows a received signal response sampled over 512 samples. The variance box will take the average of these nine values and calculate the variance of all eighty-one pixels. Thus a strong variation would automatically show up and one would have the detected object.

The algorithm has been divided into the following parts or sections:

- Convert the raw images into ASCII images (readable by MATLAB),
- Perform background removal,
- Strip off initial error,
- Divide the image into m-by-n cells,
- Calculate the sum, mean and variance of each cell,
- Identify the maximum value of the variance matrix,
- Draw the bounding box,
- Nearest neighborhood detection and locate the local maxima,
- Identify the pipes, and
- Display the location of pipes.

Air-Surface interaction produces a very high difference in permittivity. This causes a high reflection which shows up at the top of all GPR images. We employ a method called as Background Removal. This gets rid of the ringing effect of some antennas. The background algorithm which was employed here sums up all the amplitudes of reflections that were recorded at the same time along a profile and divides by the number of traces summed. This way one can get rid of the aberrant reflections at the top as well as the ringing effect which might have caused removal of the good data.

Rail ties are a special case for GPR systems. They occur at very regular intervals, are located very close to ground and radar signals have to pass through them to get to the subsurface. Simple background removal techniques do not work on the rail ties. For the purposes of the same, different techniques might be used:

- Averaging out the data received from the tracks (at the tie level) and applying a common mean value at that segment of the data.
- Applying negative gain at the tie level and applying positive gain to the sections below so as to amplify the points where our objects might be present.
- Ignoring any detected objects at the top of the image (which relate to rail-ties).

The relationship between the transmitted power, received power, the distance between the receiving antenna, size of the reflecting object, speed of propagation and the frequency of operation can be given by $PR = F(R,D,v,f)$ where

R = Distance between the antenna and object
D = Diameter of object
V = Velocity of the approaching object (Speed of the antenna)
f = Frequency of the Antenna.

It indicates that if at a particular point in the receiving matrix we have higher amplitude, there will be a higher variance around that area. The receiving power of the antenna is the power which is visible on the visual display unit. Now as the antenna is approaching the object, there is a distinct increase in the energy being received back, indicated by the apex of the parabola.

The ideology behind the algorithm is that the pipes or relevant objects will have the highest intensity amongst all the pixels. After dividing the image into m by n pixels, sum, mean and variance of each cell is calculated. What we obtain is an x/m by y/n sized matrix. Each pixel represents the variance of the entire

cell. Each pixel size is representative of m by n cell size and shows the cell variance.

To detect if any overlapping has occurred, one needs to define a bounding box which encompasses p by q percent of the entire variance matrix. The bounding box contains all pixels around the brightest spot. If an object is present around a larger object it will be left out as its intensity will be invariably be less than of the larger, more dominant object. The next step is to shrink the box. The pixels in the bounding box are divided to form a gradient, which is in a histogram of the pixel intensities, and shrink the bounding box to only account for the pixels having intensity more than a particular threshold.

Once the approximated region of local maxima has been located, one needs to locate it. This is the brightest value pixel in the matrix, which is the approximate location of the object.

To compare the object location with the original file, one has to extrapolate the variance matrix to the original matrix. Figure 2 shows a representative sample of the extrapolated file. As seen in Figure 2, the actual location of the object and the blue check marks are displaced by a certain amount. This is a built-in error which can be reduced to a large extent by use of a multiplication factor. The errors and the error reduction are discussed in the conclusion.

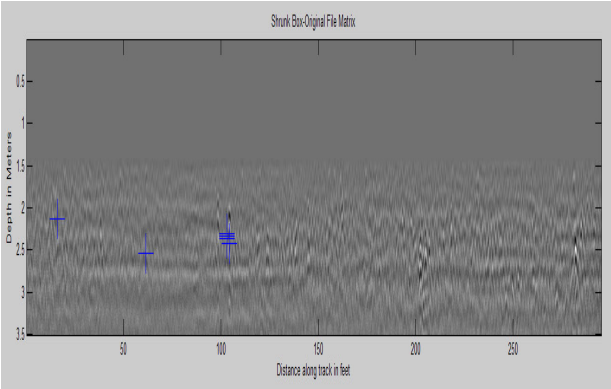

Figure 2: Some objects detected in the original preprocessed GPR image.

3. Detection Results Analysis

For the purpose of experimentation a section of Arbor Rail Line track was chosen [8]. The following results show the experimental results. Figure 3 shows pipe detection algorithm as applied to the first section of track (from Landmark 1 to landmark 4).

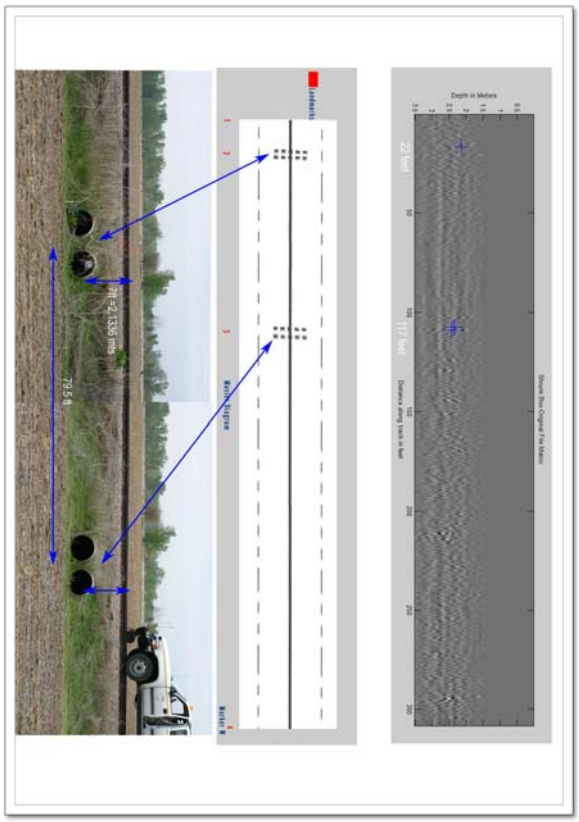

Figure 3: Pipes Detected from Pipes 1 to 4 and Landmarks 1-4.

Figure 4 shows the detection algorithm when applied to the second section of the track. That is from landmark four to land mark eleven. It has eight pipes and the GPR data is shown in Figure 5. Some of the observations which were noticed from the algorithm are:

• 83 % detection rate,
• Depth of all the pipes are detected perfectly,
• Horizontal location of the pipes is not perfect. This occurs because the speed of travel for the entire algorithm is taken to be constant.
• Aberrant detection occurs at landmark nine. There may be two reasons for the misdetection. (a) Higher threshold: A higher threshold will cause misdetection, this can happen when the pipes we are looking for are located deep and do not have the same reflection intensity as the ones with a higher reflectivity. (b)

Large variation is speed, which might have caused an aberrant detection at 475 feet.

• Multiple detection at some of the pipes locations. This can happen as the size of the pipe is large and the size of the detection square is small.

4. Conclusion

The aim of the project was to detect object with a high degree of certainty. The algorithm was able to detect most of the subsurface objects and it will work for most of the pipe-like objects. Despite some of the discrepancy in the (horizontal) location of the pipes, the algorithm was able to detect the exact depth (vertical location) of the pipes within a few inches. As explained the horizontal variation occurs as one is trying to exactly locate the pipes based on an average speed, where as the speed is not constant and varies. The high variation causes discrepancy and can be removed by better data collection methods.

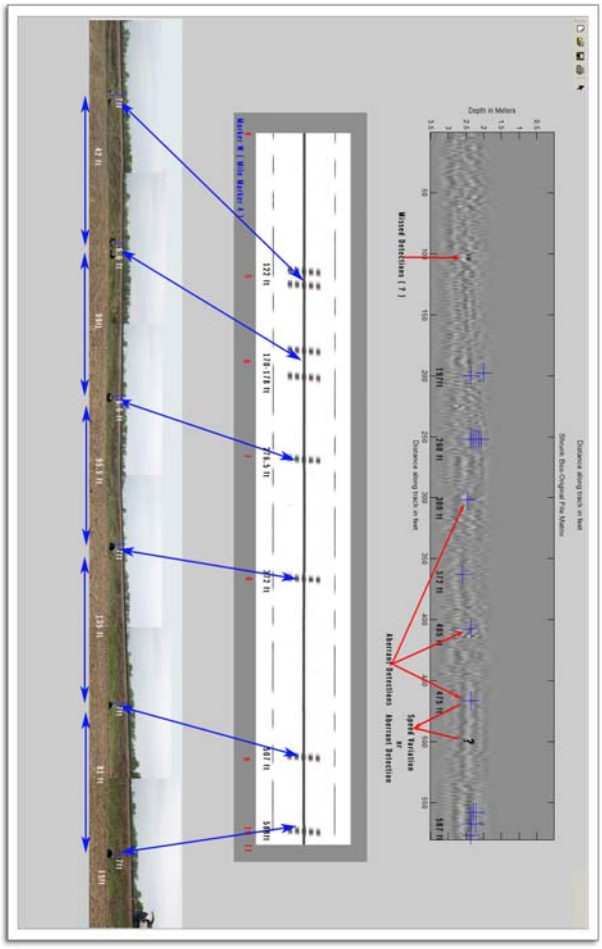

Figure 4: Pipes detected from Landmarks 5-11.

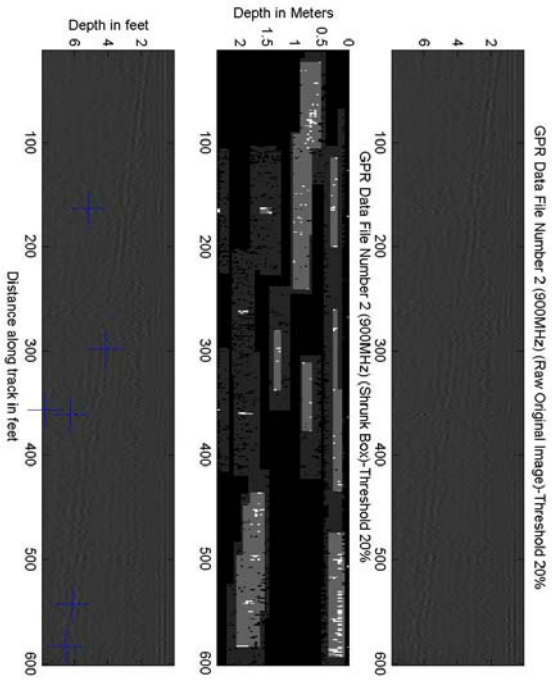

Figure 5: GPR data of detected pipes in figure 4.

References

[1] Gary, “www.g-p-r.com,” www.g-p-r.com, 2000.

[2] Federal Railroad Authority, “Train accidents by specific cause and type,” 2002, Table 5.9 of the Publication by Federal Railroad Authority.

[3] Allan M Zarembski, “Using radar to investigate roadbed,” Railway Track and Structures, vol. 84, no. 12, pp. 16–17, December 1988.

[4] Chris J. Kumke, “Railroad track substructure monitoring using ground penetrating radar,” Masters thesis, University of Nebraska, Lincoln, September 1999.

[5] Paik Joonki; P. Lee Cheolha; and A. Abidi Mongi, “Image processing based mine detection techniques: A review,” Subsurface Sensing Technology and Applications, vol. 3, no. 3, pp. 153–202, 2002.

[6] Geophysical Systems, “www.geophysical.com,” 2004.

[7] S.A Arcone, “Numerical studies of the radiation patterns of resistively loaded dipoles,” Journal of Applied Geophysics, vol. 33, no. 1-3, pp. 39–52, 1995.

[8] Omaha Public Power District, “Arobor rail line,” Autocad Design, February 2003.